

Torrefaction of spelt husks to upgrade its physicochemical properties

Halidu A, Bilsborrow PE, Phan AP*.

Abstract

Biomass conversion to energy has taken centre stage to achieve net zero carbon footprint. Although its usage poses a significant challenge that needs to be addressed. In this study, torrefaction of spelt husk was carried out to improve its physicochemical properties for further utilization in the gasification system. The torrefaction process was carried out at 200, 250 and 300°C under a nitrogen environment at a residence time of 15, 30, 45 and 60 mins respectively. The results showed that the energy density (HHV) was increased with increasing torrefaction temperature as well as there was enhanced grindability which indicates the weakness in brittleness and fragility of the torrefied spelt husk which would otherwise facilitate storage and transportation.

Introduction

Energy from biomass has increasingly become attractive due to the availability of biomass in all parts of the world. Biomass have low energy density, high moisture content, low heating value as such becomes a key challenge for biomass transportation, storage and very difficult to be used directly during pyrolysis, gasification and liquefaction processes (Kai *et al.*, 2017; Xia *et al.*, 2018; Yang *et al.*, 2018). Another challenge for biomass commercial usage in the pyrolysis or gasification reactors is the acidity and corrosivity of its crude bio-oil (Czernik and Bridgwater, 2004). As such the improvement of biomass properties through pre-treatment process such as torrefaction is a way in solving the challenges mentioned. Torrefaction is referred to as mild pyrolysis of biomass at temperatures between 200 to 300°C in an oxygen-free environment in order to increase its heating value, enhanced grindability and storability which can be used as a pre-treatment for other thermochemical processes (Sukiran *et al.*, 2017; Kai *et al.*, 2019). Previous studies on torrefaction of biomass have revealed an improved fuel properties which made it suitable for gasification process (Zhang *et al.*, 2020). Research have showed that torrefaction of rice husk enhanced its fuel properties due to the removal of its oxygen content (Chen *et al.*, 2018). In another related studies, torrefaction of wood led to easy grindability and low moisture content of biomass thereby making the hydroxyl functional groups of the biomass to be destroyed (Arias *et al.*, 2008). In a studies by Zhang *et al.* (2015), the oxygen content of rice husks greatly declined following torrefaction at 280°C for 10 mins from 38.59% to 27.68% whereas its high heating value increased from 16.58MJkg⁻¹ to 18.73MJkg⁻¹ respectively. Most literatures on torrefaction of biomass focused on the solid products otherwise known as biochars and very little literatures on the liquid and gas products, whereas torrefaction products consist of both solid, liquid and gas. However, the studies on the torrefaction of corn stover revealed that the liquid products contains majorly ketones, aldehydes, furan derivatives, phenolic and organic acids (Ren *et al.*, 2014). In a similar studies carried out on bamboo by Chen *et al.* (2015b) which was torrefied at 250 to 350°C under a residence time of 30 to 90mins, the liquid product also contained rich amount of acids, ketones, phenols, aldehydes, esters and alcohols and 50% of water with a pH range of 2.27 to 2.60 which is closer to that of bio-oil (2.5). Previous researchers have focused their studies on the mass loss of biomass during torrefaction and the effect of process conditions on the chemical properties of the product. Less attention has been paid to the grindability or the surface morphology of torrefied biomass. In this study, the torrefaction of spelt husks was performed at 200, 250 and 300°C under an inert nitrogen environment at 20°C.min⁻¹ heating rate with a residence time of 15-60min, respectively. The effect of torrefaction temperatures and residence time on the yields and properties of torrefaction products were analysed. These range of torrefaction parameters were reported in the literature for different biomass materials (Zhang *et al.*, 2019; Tong *et al.*, 2020). The FTIR and

SEM-EDX analysis of the solid product was performed. The GC-MS, water content and pH analysis of liquid product was also carried out in order to understand the chemical composition for further utilization of the torrefied spelt husks.

Materials and methods

Spelt husks was obtained from a local organic flour mill based in Stamfordham, Northumberland.

Experimental procedure

The torrefaction experiment using spelt husks was carried out in a stainless steel reactor as shown on Fig. 1.0 which has an internal diameter of 14cm and a height of 28cm in which 40g (±0.5) of the biomass was fed and then heated to a preferred temperature of 200, 250 and 300°C respectively. A heating rate of 20°C min⁻¹ was used under a nitrogen flow rate of 60cm³ min⁻¹ to eliminate ignition and oxidation. The sample was held for a duration of 15-60 mins as the residence time for each desired torrefaction temperature. After the process, the non-condensable gas samples were collected using gas bags in triplicates for gas chromatography (GC) analysis as described in a previous study (Prasertcharoensuk *et al.*, 2019) and the solid products where collected from the reactor cooled to a temperature of less than 50°C, whereas the liquid products were collected from the condenser which was kept at 0°C immersed in an ice bath. The samples were collected to determine char yield, liquid yield, gas yield, proximate analysis and HHV and subsequently analyzed for grindability and SEM-EDX. The product yields (char, liquid and yields), enhancement factor and energy yields were calculated using the following equations by (Chen *et al.*, 2020):

$$\text{Char yield (\%)} = \frac{\text{mass of torrefied sample}}{\text{initial mass of non torrefied sample}} \times 100 \tag{1.0}$$

$$\text{Liquid yield (\%)} = \frac{\text{mass of liquid sample after torrefaction}}{\text{initial mass of non torrefied sample}} \times 100 \tag{1.1}$$

$$\text{Gas yield (\%)} = 100 - \text{char yield} - \text{liquid yield} \tag{1.2}$$

$$\text{Calorific value/Enhancement factor (EF)} = \frac{\text{HHV of torrefied sample}}{\text{HHV of non torrefied sample}} \tag{1.3}$$

$$\text{Energy yield (\%)} = \text{char yield (\%)} \times \text{EF} \tag{1.4}$$

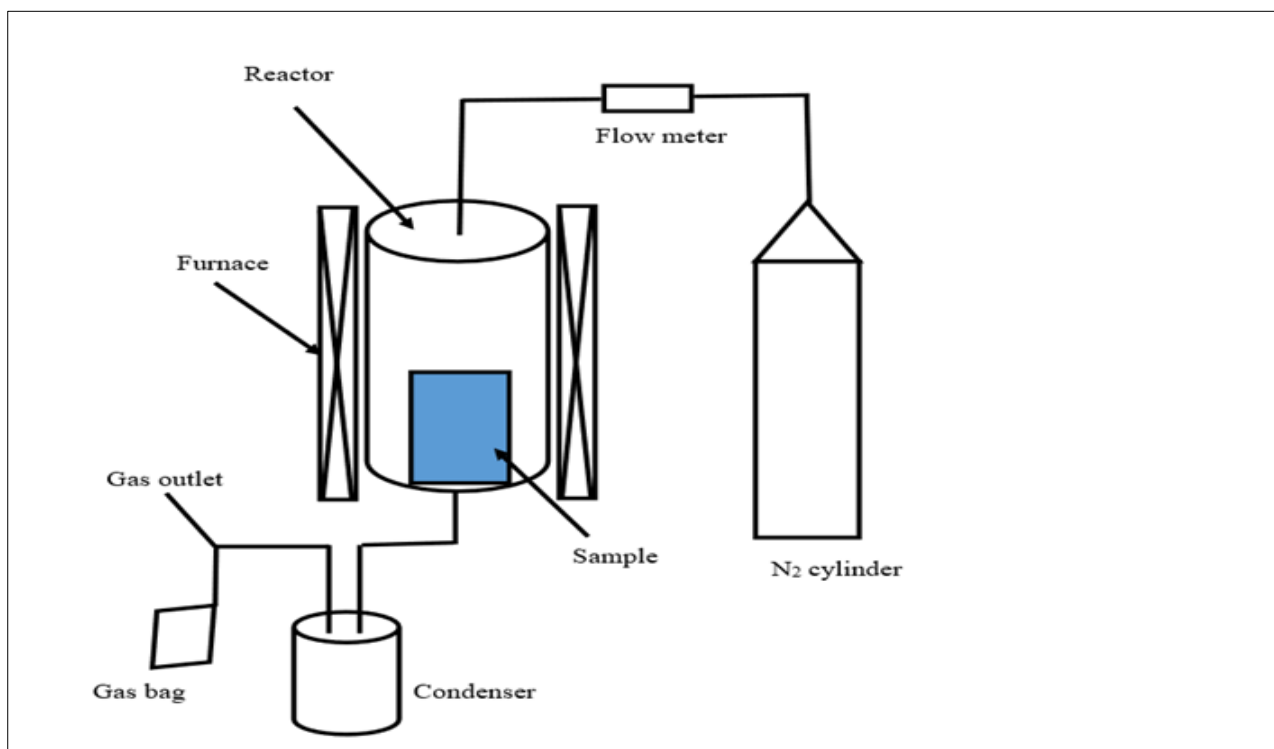


Fig. 1.0 Experimental set-up for torrefaction (Okot, 2019).

Table 1.0 Fuel properties of Spelt husk

Property	Spelt husk
<i>Proximate analysis (dry basis)</i>	
Ash content (% wt)	7.07 (± 0.13)
Volatile (% wt)	81.96 (± 0.07)
Fixed carbon(%wt) by difference	10.97 (± 0.20)
<i>Ultimate analysis (dry and ash free)</i>	
C (%)	48.61 (± 0.11)
H (%)	6.40 (± 0.06)
N (%)	2.30 (± 0.00)
O* (%) by difference	42.69 (± 0.17)
High heating value (HHV) (MJkg ⁻¹)	17.56 (± 0.08)
Low heating value (LHV) (MJkg ⁻¹)	16.21 (± 0.02)
<i>Fibre analysis</i>	
Cellulose (%)	12.12
Hemicellulose (%)	12.57
Lignin (%)	9.81
Extractives (%)	65.50
<i>Inorganic composition ($\mu\text{g/g}$)</i>	
K	5315.0
P	297.4
Mg	716.5
Ca	3820.5
Zn	47.4
Fe	47.1
Mn	50.5
Cu	15.9
<i>Inorganic composition ($\mu\text{g/g}$)</i>	
Al	106.3
Ba	11.6
Sr	11.2
B	2.0
Na	146.4
Rb	4.4
Ni	1.5
Co	nd
Si	nd
P	297.4
Mo	0.7
Sc	0.2
Ti	4.8
V	0.3
Cr	2.2
Ga	1.4
Ge	nd
As	0.7
Se	0.6
Y	0.1
Zr	1.5
Nb	nd

La	0.1
Ce	0.2
Pr	nd
Nd	0.2
Hf	0.1
Os	4.7
Au	1.1
Pb	0.7

Sample analysis

The fibre analysis (hemicellulose, cellulose, and lignin), proximate analysis (BS1016-6) ultimate analysis, HHV, and scanning electron microscopy (SEM) analysis of spelt husk and torrefied biomass were carried out as described in previous studies of Okot *et al.* (2019) whereas the pH and water content of the liquid product was performed as described by Prasertcharoensuk *et al.* (2019). Fourier transformed infrared radiation (FTIR) analysis of liquid and solid products (grounded to 0.25 mm size) was performed using Cary 630 FTIR with an image range of 600 to 4000 cm^{-1} to identify the functional groups at various intensities. The gas composition was analysed by the Varian 450 GC with thermal conductivity detector (TCD) and flame ionisation detector (FID). The gas chromatography (GC) comprises of two ovens with the first oven housing 3 columns (Hayesep T0.5mx1/8" ultimet, Hayesep Q0.5mx1/8" ultimet and Molsieve 13X1.5mx1/8" ultimet) for permanent gas detection. The second oven had two columns: the CP-SIL 5CB FS25X.25 (0.4 mm ID) for the detection of hydrocarbons and CP-WAX 52CB FS 25X.32 (1.2 mm ID) for the detection of oxygenated compounds. The first oven was kept at a temperature of 100°C, while the second oven temperature varied from 40-120°C, i.e. an initial temperature of 40°C, kept for 2 minutes; 40- 50°C at a heating rate of 0.5°C min^{-1} ; 50-100°C at a heating rate of 8°C min^{-1} , 100-120°C at a heating rate of 10°C min^{-1} . The chemical compositions of the liquid samples were recognized and measured using a 7200 Accurate-Mass Q-TOF GC/MS and gas chromatography flame ionization detector (GC-FID) equipped with a 60 m \times 250 μm \times 0.25 μm capillary column (14%-cyanopropyl- phenylmethylpolysiloxane, Restek Rtx-1707) with helium as carrier gas.

Results and Discussion

Influence of torrefaction on the products yield

Figs. 4.1, 4.2 & 4.3 shows the char yield, liquid yield, and gas yield of torrefied raw spelt husk at varying reaction temperatures and residence time. The loss of mass which is measured in terms of char yield (Fig. 4.1) in the spelt husk may be due to the release of moisture and volatile matter. During torrefaction, moisture content was released by two separate mechanisms. The first process was the evaporation of the moisture content of biomass which showed a decreasing trend (Table 3.2) and the second was the dehydration of organic biomass components as reported by (Chen *et al.*, 2014). The predominant factor that affected the product yields was temperature presumably attributed to enhanced devolatilization of lignin, cellulose, and hemicellulose above 250°C as reported by Medic *et al.* (2012). The char yield varied from 54.80% (± 2.22) at 300°C and 60 min to 91.66% (± 0.80) at 200°C and 15 min as can be seen in Fig. 4.1, the liquid yield vary from 2.16% (± 1.63) at 200°C and 15 min to 24.87% (± 1.74) at 300°C and 60 min, while the gas yield also follow the same trend and has the lowest gas yield at 200°C and 15 min (6.18% ± 0.82) and the highest gas yield was obtained at 300°C and 60 min (20.33% ± 2.45) respectively. As observed by the figures below, there was an overall trend in decrease in char yield and increase in liquid yield and gas yield as the process parameters increases. The loss in the char yield was much more pronounced at temperatures between 250 – 300°C than between 200 – 250°C. The mass loss (char yield) between 250 – 300°C was probably due to the higher reactivity or may be due to more extensive devolatilization and decarbonisation of hemicellulose fraction above 250°C. Medic *et al.* (2010) also reported the same trend of mass loss (char yield), liquid yield and gas yield which they attributed to

the degradation of hemicellulose and initial reactions of cellulose decomposition which may have occurred at that temperature regime. Ahiduzzaman and Islam (2015) conducted a study on the energy yield of torrefied rice husk and he also reported the same trend of results for mass yield. Studies from Felfli *et al.* (2005) and Almeida *et al.* (2010) also reported the same trend which they attributed it the likelihood of more extensive decomposition of not only hemicellulose but also the thermal decomposition of some short chain lignin compounds and the decomposition of the fraction of polymer present in the biomass. Similarly, studies on the torrefaction of food waste by Pahla *et al.* (2018) where the char yield declines as the torrefaction temperature increases from 200 to 300°C. In another related studies by Zheng *et al.* (2013), when the residence time was increased from 10 to 60 mins at a torrefaction temperature of 275°C, it was found that there was a reduction in the char yield from 88.14 to 80.13%. The findings agreed with that of torrefaction of feedstock from food waste (Poudel *et al.*, 2015), beech wood chip (Colin *et al.*, 2017) and rice husk (Chen *et al.*, 2018). The colour of the torrefied spelt husks became darker with rise in torrefaction temperature possibly due to increase in carbonisation (Fig. 4.1). Related colour changes were also reported for rice husk (Chen *et al.*, 2014). Studies from Felfli *et al.* (2005) and Almeida *et al.* (2010) also reported the same trend which they attributed it the likelihood of more extensive decomposition of not only hemicellulose but also the thermal decomposition of some short chain lignin compounds and the decomposition of the fraction of polymer present in the biomass. Similarly, studies on the torrefaction of food waste by Pahla *et al.* (2018), the char yield declines as the torrefaction temperature increases from 200 to 300°C. In another related studies by Zheng *et al.* (2013), when the residence time was increased from 10 to 60 mins at a torrefaction temperature of 275°C, it was found that that there was a reduction in the char yield from 88.14 to 80.13%.

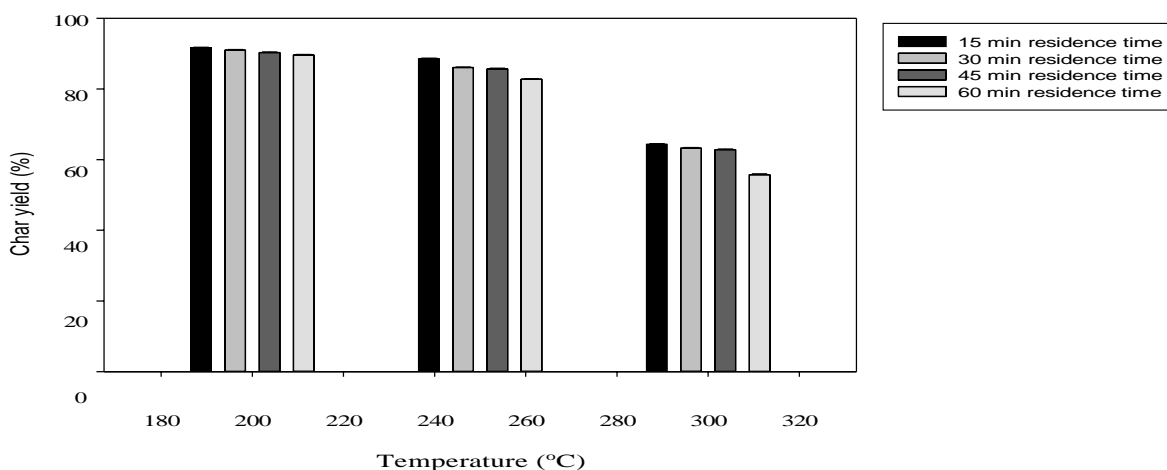


Fig.4.1 Char yield of torrefied spelt husk at varying temperature and residence time

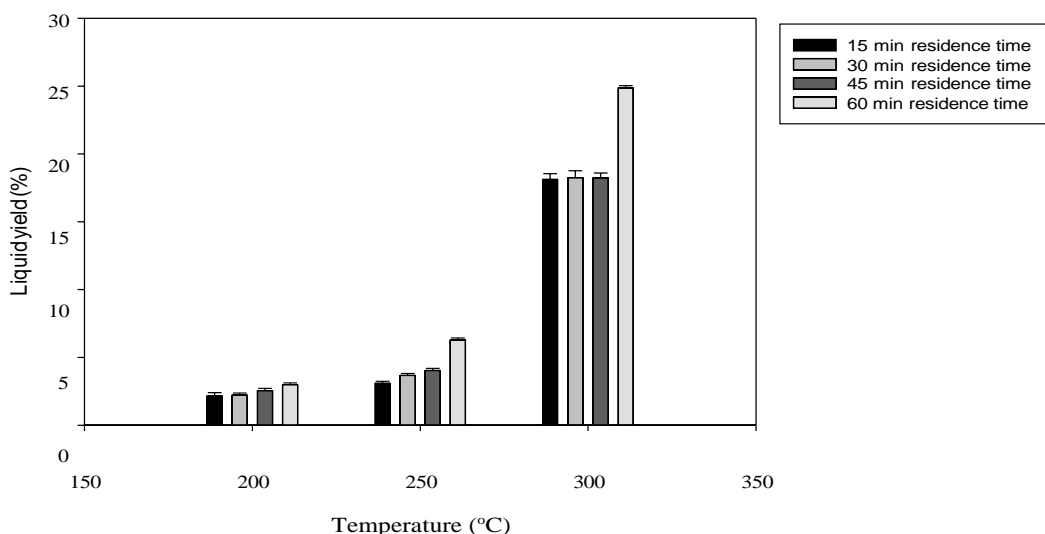


Fig. 4.2 Liquid yield of torrefied spelt husks at vaying temperature and residence time

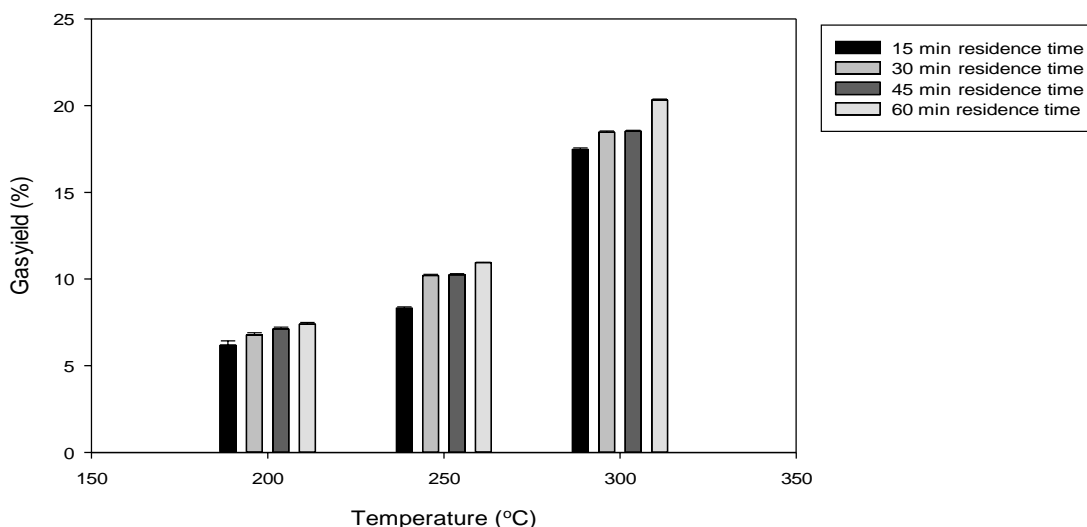


Fig. 4.3 Gas yield of torrefied spelt husks at varying temperatures and residence time

Energy yield is an indication of the enhancement of calorific value of spelt husk by torrefaction process and it is an important parameter in defining the quality of fuel in any biomass that has undergone torrefaction. Fig. 4.4 shows the influence of torrefaction parameters (temperature and residence time) on the energy yield of torrefied spelt husk. The energy yield ranged from 84.79% to 96.96%. Generally, the energy yield decreases as the temperature and residence time decreases except that at 250°C and 15 min where the energy yield is the highest (96.96%). In a studies conducted on torrefied rice husk by Ahiduzzaman and Islam (2015), the energy yield at 250°C and 10 min (98%) was relatively similar to this studies on torrefied spelt husk. The trend of the energy yield is similar to that of the char yield which indicates that solid yield is the principal feature in determining the energy yields as reported by Ho *et al.* (2018). Torrefaction decreased the oxygen content but raised the carbon content of the spelt husk, thereby increasing the heating value of the spelt husk by increasing the temperature. As seen in the Fig. 4.4, the energy yield showed a similar pattern to that of char yield, both of which decreased with an increase in torrefaction temperature. The temperature had a more pronounced effect on the char yield relative to the energy yield. When the torrefaction temperature was below 250°C, the energy yield was more than 89%. When it was higher than 250°C, most hemicelluloses were decomposed and cellulose began to decompose, resulting in a rapid decay of char yield, while the HHV of torrefied spelt husk did not increase significantly. As a result, the energy yield fell rapidly. At 300°C with a residence time of 30 mins, the energy yield was just 73.50% (Table 3.2) which is similar to that of rice husk torrefied at 300°C for a residence time of 30mins as reported by (Chen *et al.*, 2014).

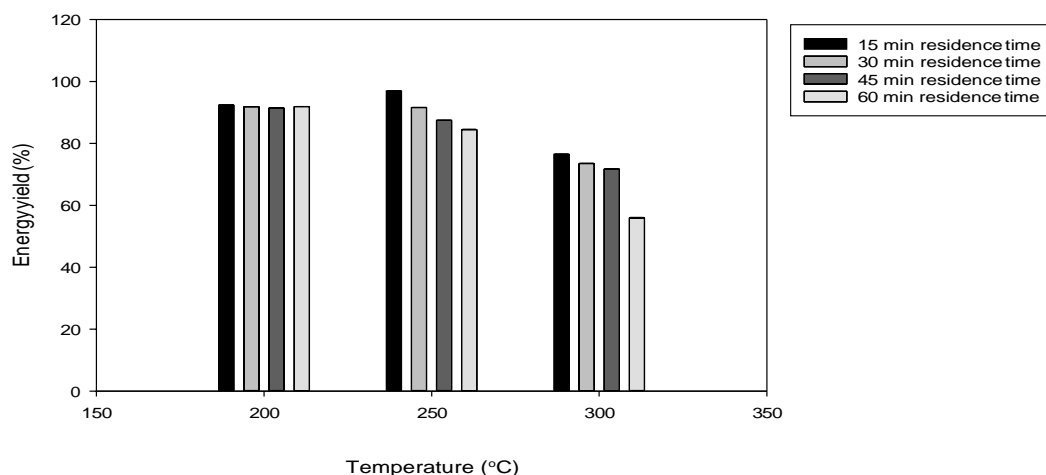


Fig. 4.4 Energy yield of torrefied spelt husk at varying temperatures and residence time

Influence of torrefaction on energy yield of spelt husk

Char properties

It can be seen from Table 3.2 that with increasing torrefaction temperature, the volatile matter content decreases with respect to residence time. However, the decrease was much apparent at torrefaction temperatures between 250 to 300°C irrespective of the residence which indicates that torrefaction temperature had more influence on the volatile matter. Similar observations were made by studies on torrefaction of rice husks by Chen *et al.* (2014), Phanphanich and Mani (2011) (pine chips torrefaction) and Ohliger *et al.* (2013) (torrefaction of beechwood chips). Contrastingly, increase in torrefaction temperature led to increased inorganic compounds (ash content) in the biomass as shown in Table 3.2 which remained as char fraction at the studied temperatures 200 to 300°C, as the volatiles are released leading to an increase in the ash content of the torrefied spelt husk which remained in the char. The fixed carbon content in the torrefied spelt husk also increased with an increase in torrefaction temperature from 200 to 300°C. As can be seen in Table 3.2 with increasing torrefaction temperature with respect to the residence time, the ultimate analysis which showed main elements such as carbon, hydrogen, nitrogen, and oxygen changed to various degrees. Hydrogen content was basically not reduced at torrefaction temperatures between 200 to 250°C with only slight reduction been detected but when the torrefaction temperature was increased from 250°C to 300°C which was probably due to hydrocarbons such as methane (CH₄) and ethane (C₂H₆) are only released at higher temperatures. Similar results have been reported for torrefied rice husk (Chen *et al.*, 2014). The noticeable change is the carbon and oxygen contents. Carbon content steadily increased, and the oxygen content of the torrefied spelt husk experienced a considerable decrease. This was because spelt husk went through decarboxylation and carbonylation reactions during the torrefaction, producing moisture, CO₂, CO, and oxygen-comprising carbohydrates. Park *et al.* (2013) in their studies on the transformation of loblolly pine chips during torrefaction recommended that the changes in the contents of carbon and oxygen are due to the production and release of CO₂ and CO during torrefaction process.

Fourier transform infrared spectroscopy (FTIR) analysis of bio-char from torrefaction

The FTIR was used to analyse the chemical composition of raw spelt husk and three bio-char samples from torrefaction of spelt husk at 200, 250 and 300°C torrefaction temperature with a residence time of 30 minutes respectively. Table 3.4 shows the wavenumbers of functional groups that are present in raw biomass and bio-char while Fig. 4.5 displays the FTIR spectra of raw spelt husk and bio-char samples. Fig.4.5 are defined by the respective main intensities. The intensity of O-H group at 3200 -3600 cm⁻¹ (water, alcohol, and phenol) are present in both the raw spelt husk and the bio-chars as also reported by (Wei *et al.*, 2015), whereas the weaker bond wavenumbers

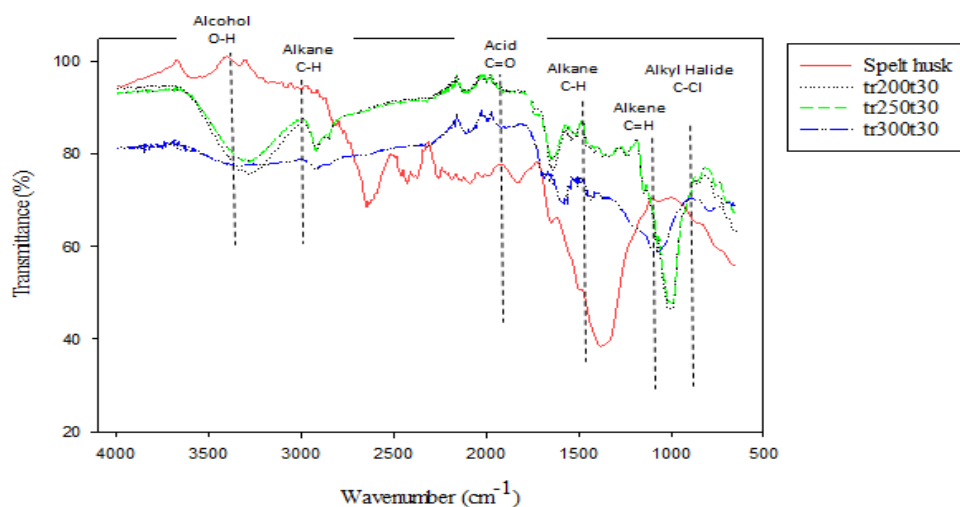


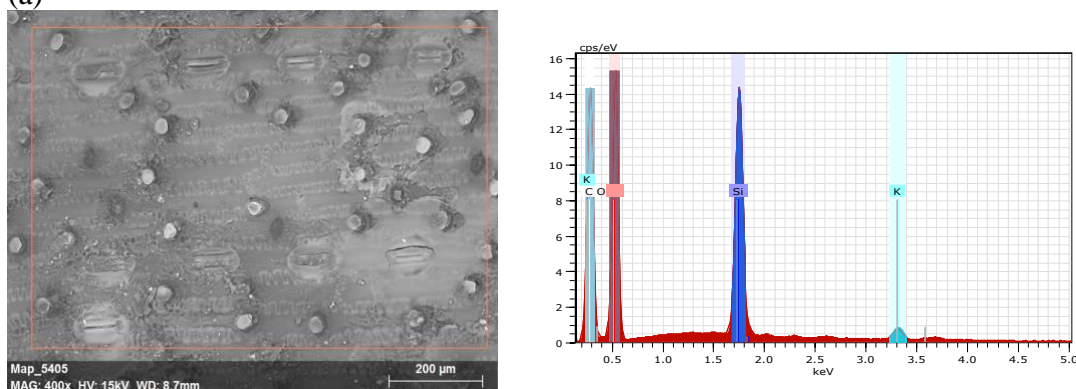
Fig. 4.5 FTIR spectra of raw spelt husk and biochar torrefied at different temperatures for a residence time of 30 min

such as 1400–1620, 1000–1300, 600–1000 and 500–600cm⁻¹ for the stretching vibrations of the C = C, C – O, = C – H and C – Br groups, suggest the presence of functional aromatic, ether, alkene and alkyl halide groups, respectively. These vibrations are expected from hemicelluloses, cellulose, and lignin and are consistent with the findings documented by (Joshi *et al.*, 2015).

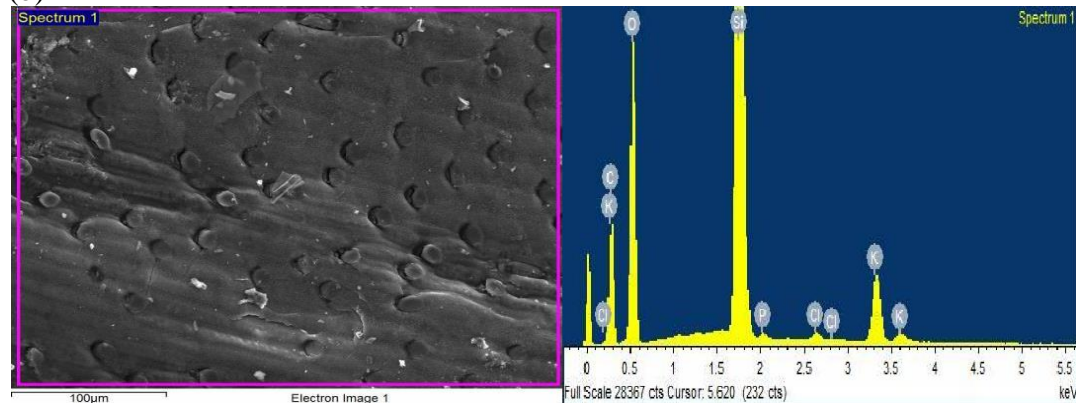
SEM images and EDX Analysis

SEM – EDX methodology has been used on samples of biomass to obtain an understanding of the textural properties and morphology of the biomass samples and then, when torrefaction is applied, the structural changes occur on those samples. From Fig. 4.6 below it is evident and visible that the raw biomass which is the parent material are made of solid bridge cells which are enhanced by the mechanical interlocking of the bonds between the particles which is typical of lignocellulosic structure. The raw spelt husk and the bio-chars showed identical SEM images. SEM images from various biomass parts showed that the internal portions of these channels are also filled and raw makers are originally not porous. SEM image of bio-chars obtained from torrefaction showed a strong dependence on torrefaction temperatures which had a disorganized rough surface morphology as the applied torrefaction temperature increases from 200, 250, to 300°C indicating that the original lignocellulosic structures were destroyed. The findings of EDX (Fig.4.6) are identical with high oxygen and carbon contents, and mineral matter for both samples was also detected. Silicon, potassium, phosphorus, and chlorine are essential elements other than carbon and oxygen.

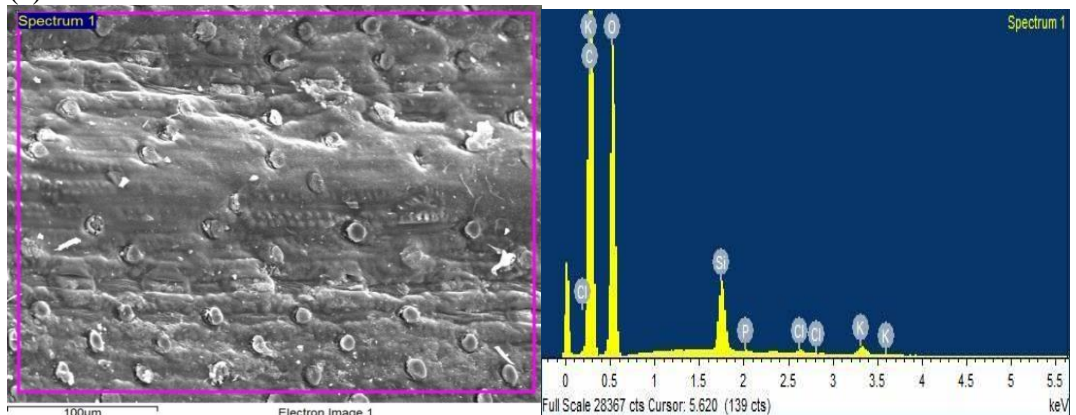
(a)



(b)



(c)



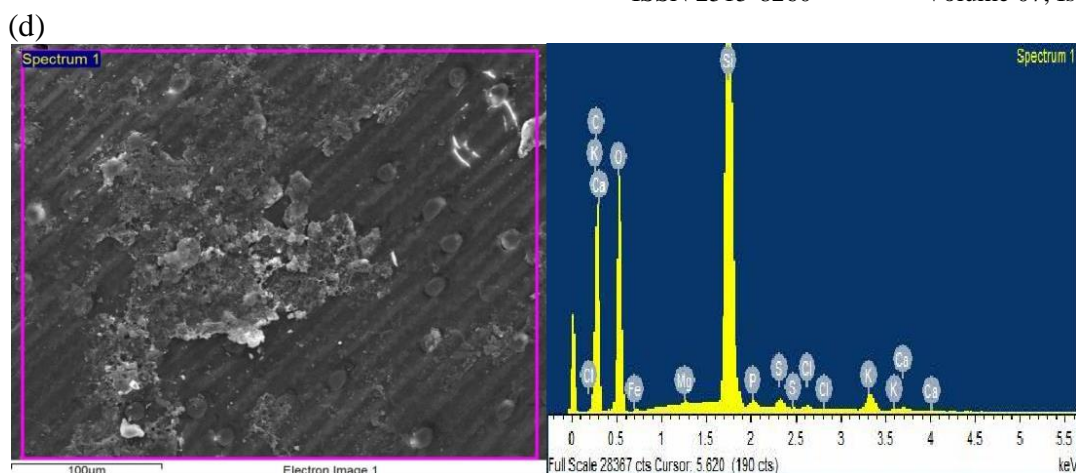


Fig. 4.6 SEM images and EDX of (a) spelt husk and bio-chars at torrefaction temperatures of (b) 200°C, (c) 250°C, (d) 300°C at a residence time of 30 mins.

Grindability

The grindability of the raw and torrefied spelt husks was measured in terms of particle size distribution. Raw and torrefied spelt husks measured in a 200cm³ cylinder was grinded using a HGBTWTS3 laboratory blender 8010ES at a fixed grinding period of 20s and then segregated using screen sizes from 1.00 to 4.00 mm sieves with a Retsch sieve shaker AS 200 at a fixed sieving time of 10 min. The table below (Table 3.5) shows the grindability of the torrefied spelt husks at different torrefaction temperature and residence time. The increase in the grindability with respect to increase in the torrefaction temperature is linear as it is evidence by a rise in the fine particles (<1.00mm) which leads to less energy requirement. During torrefaction as reported by Chen *et al.* (2015a) the fibre structure of the feedstock is weakened as a result of difference in the thermal stabilities of hemicellulose, cellulose and lignin which makes biomass materials more brittle and breakable. Although the residence time had effect on the grindability too as such the torrefied spelt husk had higher grindability than the raw spelt husks which decreased the cost of feedstock grinding as reported by (Chen *et al.*, 2015a) in their work on the torrefaction of cotton stalk.

Table 3.2 proximate analysis, high heating values and energy yield of torrefied spelt husk

Residence time (min)	Volatile (wt.%, db)			Ash (wt.%, db)			Fixed carbon ^a (wt.%, db)			HHV (MJkg ⁻¹)			Energy yield (%)		
	200 °C	250 °C	300 °C	200 °C	250 °C	300 °C	200 °C	250 °C	300 °C	200° C	250° C	300° C	200 °C	250 °C	300 °C
15	74.58	72.94	70.29	3.62	3.74	5.46	21.80	23.32	24.25	17.7	19.2	20.8	92.39	96.99	76.54
30	74.30	71.91	69.63	3.67	4.05	5.89	22.03	24.04	24.48	17.7	18.6	20.4	91.84	91.55	73.50

45	73. 65	71. 22	68. 52	3.6 9	4.5 2	5.9 6	22. 66	24. 26	25. 52	17.7 7 (±0. 13)	17.9 1 (±1. 33)	20.0 3 (±0. 30)	91. 40	87. 42	71. 71
60	73. 20	70. 89	67. 37	3.7 1	4.8 3	6.0 3	23. 09	24. 28	26. 60	18.0 1 (±0. 07)	17.9 2 (±1. 43)	17.9 3 (±0. 50)	91. 90	84. 46	55. 95

db= dry basis; ^a=by difference

Table 3.3 Ultimate analysis of torrefied spelt husk (max S.E. ±0.09)

Residence time (min)	Carbon (% , daf)			Hydrogen (% , daf)			Nitrogen (% , daf)			Oxygen ^b (% , daf)		
	200°	250°	300°	200°	250°	300°	200°	250°	300°	200°	250°	300°
15	43.79	44.90	56.26	6.66	6.66	5.75	1.99	2.14	2.28	49.38	48.23	39.09
30	43.88	46.45	58.43	6.51	6.60	5.62	1.97	2.05	2.69	49.49	47.05	37.03
45	43.90	48.11	66.76	6.48	6.55	4.65	1.94	1.96	2.26	49.54	45.86	30.59
60	43.92	49.69	75.10	6.45	6.48	3.66	1.92	1.86	1.83	49.58	44.68	24.16

daf= dry ash free; ^b= by difference

Table 3.4 FTIR functional groups and frequency for bio-char (Kotaiah Naik *et al.*, 2017)

wavenumber(cm ⁻¹)	Type of vibration	Name of the functional group
3200–3600	O–H (stretch, H-bonded) strong, broad	Alcohol
2850–3000	C–H stretch strong	Alkane
1700–1725	C=O stretch strong	Acid
1550–1640	N–H bending	Amide
1400–1600	C=C stretch medium-weak, multiple bands	Aromatic
1350–1480	C–H bending variable	Alkane
1210–1320	C–O (stretch) strong	Acid
1050–1150	C–O (stretch) strong	Alcohol
675–1000	C=C bending strong	Alkene
600–800	C–Cl stretch strong	Alkyl halide

Table 3.5 Grindability of biomass torrefied at temperature of 200-300°C and holding time of 15- 60min. Maximum error in grindability was ± 2.96 % wt

Residence time (min)	Temperature (°C)	Spelt husks (% wt)			
		<1.00mm	1.00- <2.36mm	2.36 - <4.00mm	>4.00mm
raw	-	49.44	27.35	10.43	12.78
15	200	54.44	31.09	8.45	6.02
	250	58.44	27.77	8.12	5.67
	300	60.94	26.27	7.01	5.78
30	200	60.44	28.7	6.07	4.79
	250	62.91	27.83	6.05	3.21
	300	69.21	24.54	3.13	3.12
45	200	72.21	23.54	2.15	2.1
	250	72.42	23.67	1.99	1.92
	300	79.54	18.41	1.03	1.02
60	200	80.21	17.86	0.98	0.95
	250	82.06	16.52	0.91	0.51
	300	87.19	11.69	0.9	0.22

Liquid product analysis

The liquid obtained from the torrefaction principally contained water in a high quantity in the range of 83 to 97 wt% with a pH range of 3 to 4 which shows that it is very acidic as can be seen on Table 2. The GC-MS analysis also showed Liquid obtained from torrefaction contained mainly high water content (93-97%wt) and was very acidic (Table 3.6 and Table 3.7). GC-MS analysis (Table 3.7) shows the liquid products generally contained phenol and its derivatives which formed higher fraction followed by, furan and its derivatives, ketones, acids, esters, alcohols, sugars and aldehydes and finally the unidentified compounds which formed the least compounds. In a related studies of the torrefaction of rice husk from 210 to 300°C by Chen *et al.* (2018) revealed the similar chemical components (phenols, acids, ketones, furans and aldehydes), also a studies on the torrefaction of bamboo by Chen *et al.* (2015c) revealed a liquid containing acids, alcohols, ketones, phenols, aldehydes and esters. The decomposition of hemicellulose and cellulose helps in the formation of sugars, acid and furans in the liquid product whereas the phenols and their derivatives are formed from the thermal decomposition of lignin (Mei *et al.*, 2016; Chen *et al.*, 2018). The water content in the liquid decreased with an increase in the torrefaction temperature and residence time. The liquid product obtained from this studies is of low quality because of its high water content and acidity, it makes it undesirable fuel for energy production and can be utilized as cherished feedstocks in the petrochemical industries.

Table 3.6 Liquid analysis after torrefaction of spelt husk at various temperature and residence time

Residence time (min)	Water content (wt. %)			pH		
	200°C	250°C	300°C	200°C	250°C	300°C
15	97.02	96.28	84.91	4.0	4.0	3.0
30	97.01	94.23	83.92	4.0	3.0	3.0
45	96.98	87.35	83.36	3.0	3.0	3.0
60	96.98	85.57	82.53	3.0	4.0	3.0

Table 3.7 Chemical compositions of liquid derived from torrefaction temperature of 200-300°C and residence time of 30 min at a nitrogen flow rate of 60 mlmin⁻¹

Torrefaction temperature (°C)	200	250	300
Functional groups	wt. % (dry basis)		
Acids	2.2	1.9	1.8
Esters	0.8	0.5	0.4
Ketones	2.7	2.1	1.9
Alcohols	2.1	1.7	1.5
Aldehydes	2.1	1.9	1.7
Furan and its derivatives	2.0	2.5	2.8
Sugars	0.7	0.9	0.9
Phenol and its derivatives	8.5	9.6	9.8
unknown	0.2	0.4	0.6

Gas product from torrefaction

The influence of torrefaction temperature on the gas products composition are shown on Table 3.8. The gas products constituents composed mainly of carbon dioxide and carbon monoxide with traces of hydrogen, methane and little of other hydrocarbons. The carbon dioxide composition was greater than 76 mol % within the range of studied temperatures. The reason for the formation of principally carbon dioxide could be attributed to the decarboxylation reaction of unstable carboxyl group in the hemicellulose structure of the spelt husks as similar reasons was put forward in a study of torrefaction of sprucewood and bagasse at a varying temperatures of 260, 280 and 300°C respectively in which similar pattern of results were presented by Chang *et al.* (2012). The formation of carbon monoxide can be attributed to the secondary reactions of CO₂ with the porous char and the decarbonylation of low molecular weight carbonyl compounds formed during increase in the torrefaction temperatures from 200 to 300°C. There was a decline in the CO₂ formation as the torrefaction temperature increases with an increase in the residence time. The predominance formation of CO₂ in the torrefaction process is an added advantage because it can be utilized as a carrier gas in torrefaction as it was used by Li *et al.* (2018) in the torrefaction of corncob using CO₂. The H₂, CH₄ and C₂-C₅ yields were less than 20 mol% whereas CO content increases with an increase in the residence time (15 to 60 min) at a torrefaction temperature of 300°C. Batidzirai *et al.* (2013) reported that torrefaction itself is energy-consuming but enhanced spelt husk grinding efficiency after torrefaction could significantly save power consumption which could offset to some degree the energy consumed in torrefaction and promote large-scale biomass pyrolysis and gasification (Chen *et al.*, 2014).

Table 3.8 Gas composition from torrefaction of spelt husks.

Residence time (min)	CO ₂ (mol %)			H ₂ (mol %)			CH ₄ (mol %)			CO (mol %)			C ₂ -C ₅ (mol %)		
	200°C	250°C	300°C	200°C	250°C	300°C	200°C	250°C	300°C	200°C	250°C	300°C	200°C	250°C	300°C
15	100.00±0.00	100.00±0.00	99.87±0.35	-	-	0.13±0.35	-	-	-	-	-	-	-	-	-
30	100.00±0.00	100.00±0.00	85.69±0.35	-	-	0.36±0.86	-	-	-	-	-	13.94±0.35	-	-	0.01±0.23
45	100.00±0.00	100.00±0.00	83.33±0.35	-	-	0.39±0.35	-	-	0.04±0.35	-	-	16.23±0.23	-	-	0.01±0.23
60	100.00±0.00	100.00±0.00	80.43±0.25	-	-	0.39±2.23	-	-	0.98±0.35	-	-	18.19±0.15	-	-	0.01±0.23

Conclusion

The results of spelt husk torrefaction is found to be the same with other biomass materials such as rice husk, maize cobs, beechwood. The findings from torrefaction revealed that torrefaction temperature had more impact on the torrefaction product yields than the residence time. Char yield decreased the energy yield, while gas and liquid yields increased with higher torrefaction temperatures. Higher torrefaction temperatures led to a net decrease in volatiles, oxygen content and energy yield, while the carbon content and high heating values (energy density) increased. Torrefied spelt husk became brittle, fragile, decreased particle size, low moisture content which will make it to be stored over a long time with low risk of mold. The liquid product was mainly water and highly acidic.

References

1. Ahiduzzaman, M. and Islam, A.K.M.S. (2015) 'Energy Yield of Torrefied Rice Husk at Atmospheric Condition', *Procedia Engineering*, 105, pp. 719-724.
2. Almeida, G., Brito, J.O. and Perré, P. (2010) 'Alterations in energy properties of eucalyptus wood and bark subjected to torrefaction: The potential of mass loss as a synthetic indicator', *Bioresource Technology*, 101(24), pp. 9778-9784.
3. Arias, B., Pevida, C., Feroso, J., Plaza, M.G., Rubiera, F. and Pis, J.J. (2008) 'Influence of torrefaction on the grindability and reactivity of woody biomass', *Fuel Processing Technology*, 89(2), pp. 169-175.
4. Batidzirai, B., Mignot, A.P.R., Schakel, W.B., Junginger, H.M. and Faaij, A.P.C. (2013) 'Biomass torrefaction technology: Techno-economic status and future prospects', *Energy*, 62, pp. 196-214.
5. Chang, S., Zhao, Z., Zheng, A., He, F., Huang, Z. and Li, H. (2012) 'Characterization of Products from Torrefaction of Sprucewood and Bagasse in an Auger Reactor', *Energy & Fuels*, 26(11), pp. 7009-7017.
6. Chen, D., Chen, F., Cen, K., Cao, X., Zhang, J. and Zhou, J. (2020) 'Upgrading rice husk via oxidative torrefaction: Characterization of solid, liquid, gaseous products and a comparison with non-oxidative torrefaction', *Fuel*, 275, p. 117936.
7. Chen, D., Gao, A., Ma, Z., Fei, D., Chang, Y. and Shen, C. (2018) 'In-depth study of rice husk torrefaction: Characterization of solid, liquid and gaseous products, oxygen migration and energy yield', *Bioresource Technology*, 253, pp. 148-153.
8. Chen, D., Zheng, Z., Fu, K., Zeng, Z., Wang, J. and Lu, M. (2015a) 'Torrefaction of biomass stalk and its effect on the yield and quality of pyrolysis products', *Fuel*, 159, pp. 27-32.
9. Chen, D., Zhou, J., Zhang, Q., Zhu, X. and Lu, Q. (2014) 'Upgrading of Rice Husk by Torrefaction and its Influence on the Fuel Properties', *BioResources; Vol 9, No 4 (2014)*.
10. Chen, W.-H., Liu, S.-H., Juang, T.-T., Tsai, C.-M. and Zhuang, Y.-Q. (2015b) 'Characterization of solid and liquid products from bamboo torrefaction', *Applied Energy*, 160, pp. 829-835.
11. Chen, W.-H., Peng, J. and Bi, X.T. (2015c) 'A state-of-the-art review of biomass torrefaction, densification and applications', *Renewable and Sustainable Energy Reviews*, 44, pp. 847-866.
12. Colin, B., Dirion, J.L., Arlabosse, P. and Salvador, S. (2017) 'Quantification of the torrefaction effects on the grindability and the hygroscopicity of wood chips', *Fuel*, 197, pp. 232-239.
13. Czernik, S. and Bridgwater, A.V. (2004) 'Overview of Applications of Biomass Fast Pyrolysis Oil', *Energy & Fuels*, 18(2), pp. 590-598.
14. Felfli, F.F., Luengo, C.A., Suárez, J.A. and Beatón, P.A. (2005) 'Wood briquette torrefaction', *Energy for Sustainable Development*, 9(3), pp. 19-22.
15. Ho, S.-H., Zhang, C., Chen, W.-H., Shen, Y. and Chang, J.-S. (2018) 'Characterization of biomass waste torrefaction under conventional and microwave heating', *Bioresource Technology*, 264, pp. 7-16.
16. Joshi, G., Rawat, D.S., Lamba, B.Y., Bisht, K.K., Kumar, P., Kumar, N. and Kumar, S. (2015) 'Transesterification of Jatropa and Karanja oils by using waste egg shell derived calcium based mixed metal oxides', *Energy Conversion and Management*, 96, pp. 258-267.
17. Kai, X., Li, R., Yang, T., Shen, S., Ji, Q. and Zhang, T. (2017) 'Study on the co-pyrolysis of rice straw and high density polyethylene blends using TG-FTIR-MS', *Energy Conversion and*

Management, 146, pp. 20-33.

19. Kai, X., Meng, Y., Yang, T., Li, B. and Xing, W. (2019) 'Effect of torrefaction on rice straw physicochemical characteristics and particulate matter emission behavior during combustion', *Bioresource Technology*, 278, pp. 1-8.
20. Kotaiah Naik, D., Monika, K., Prabhakar, S., Parthasarathy, R. and Satyavathi, B. (2017) 'Pyrolysis of sorghum bagasse biomass into bio-char and bio-oil products', *Journal of thermal analysis and calorimetry*, 127(2), pp. 1277-1289.
21. Li, S.-X., Chen, C.-Z., Li, M.-F. and Xiao, X. (2018) 'Torrefaction of corncob to produce charcoal under nitrogen and carbon dioxide atmospheres', *Bioresource Technology*, 249, pp. 348-353.
22. Medic, D., Darr, M., Potter, B. and Shah, A. (2010) 'Effect of Torrefaction Process Parameters on Biomass Feedstock Upgrading', *2010 Pittsburgh, Pennsylvania, June 20 - June 23, 2010*. St. Joseph, MI. ASABE. Available at: <http://elibrary.asabe.org/abstract.asp?aid=29898&t=5>.
23. Medic, D., Darr, M., Shah, A., Potter, B. and Zimmerman, J. (2012) 'Effects of torrefaction process parameters on biomass feedstock upgrading', *Fuel*, 91(1), pp. 147-154.
24. Mei, Y., Che, Q., Yang, Q., Draper, C., Yang, H., Zhang, S. and Chen, H. (2016) 'Torrefaction of different parts from a corn stalk and its effect on the characterization of products', *Industrial Crops and Products*, 92, pp. 26-33.
25. Ohliger, A., Förster, M. and Kneer, R. (2013) 'Torrefaction of beechwood: A parametric study including heat of reaction and grindability', *Fuel*, 104, pp. 607-613.
26. Okot, D.K. (2019) *Briquetting and Torrefaction of Agricultural Residues for Energy Production*. PhD thesis. Newcastle University.
27. Okot, D.K., Bilsborrow, P.E. and Phan, A.N. (2019) 'Briquetting characteristics of bean straw-maize cob blend', *Biomass and Bioenergy*, 126, pp. 150-158.
28. Pahla, G., Ntuli, F. and Muzenda, E. (2018) 'Torrefaction of landfill food waste for possible application in biomass co-firing', *Waste Management*, 71, pp. 512-520.
29. Park, J., Meng, J., Lim, K.H., Rojas, O.J. and Park, S. (2013) 'Transformation of lignocellulosic biomass during torrefaction', *Journal of Analytical and Applied Pyrolysis*, 100, pp. 199-206.
30. Phanphanich, M. and Mani, S. (2011) 'Impact of torrefaction on the grindability and fuel characteristics of forest biomass', *Bioresource Technology*, 102(2), pp. 1246-1253.
31. Poudel, J., Ohm, T.-I. and Oh, S.C. (2015) 'A study on torrefaction of food waste', *Fuel*, 140, pp. 275- 281.
32. Prasertcharoensuk, P., Bull, S.J. and Phan, A.N. (2019) 'Gasification of waste biomass for hydrogen production: Effects of pyrolysis parameters', *Renewable Energy*, 143, pp. 112-120.
33. Ren, S., Lei, H., Wang, L., Yadavalli, G., Liu, Y. and Julson, J. (2014) 'The integrated process of microwave torrefaction and pyrolysis of corn stover for biofuel production', *Journal of Analytical and Applied Pyrolysis*, 108, pp. 248-253.
34. Sukiran, M.A., Abnisa, F., Wan Daud, W.M.A., Abu Bakar, N. and Loh, S.K. (2017) 'A review of torrefaction of oil palm solid wastes for biofuel production', *Energy Conversion and Management*, 149, pp. 101-120.
35. Tong, S., Sun, Y., Li, X., Hu, Z., Dacres, O.D., Worasuwannarak, N., Luo, G., Liu, H., Hu, H. and Yao, H. (2020) 'Gas-pressurized torrefaction of biomass wastes: Roles of pressure and secondary reactions', *Bioresource Technology*, 313, p. 123640.
36. Wei, L., Liang, S., Guho, N.M., Hanson, A.J., Smith, M.W., Garcia-Perez, M. and McDonald, A.G. (2015) 'Production and characterization of bio-oil and biochar from the pyrolysis of residual bacterial biomass from a polyhydroxyalkanoate production process', *Journal of Analytical and Applied Pyrolysis*, 115, pp. 268-278.
37. Xia, S., Xiao, H., Liu, M., Chen, Y., Yang, H. and Chen, H. (2018) 'Pyrolysis behavior and economics analysis of the biomass pyrolytic polygeneration of forest farming waste', *Bioresource Technology*, 270, pp. 189-197.
38. Yang, T., Wang, J., Li, B., Kai, X., Xing, W. and Li, R. (2018) 'Behaviors of rice straw two-step liquefaction with sub/supercritical ethanol in carbon dioxide atmosphere', *Bioresource Technology*, 258, pp. 287-294.
39. Zhang, C., Ho, S.-H., Chen, W.-H., Fu, Y., Chang, J.-S. and Bi, X. (2019) 'Oxidative torrefaction

of biomass nutshells: Evaluations of energy efficiency as well as biochar transportation and storage', *Applied Energy*, 235, pp. 428-441.

40. Zhang, S., Dong, Q., Zhang, L., Xiong, Y., Liu, X. and Zhu, S. (2015) 'Effects of water washing and torrefaction pretreatments on rice husk pyrolysis by microwave heating', *Bioresource Technology*, 193, pp. 442-448.
41. Zhang, S., Su, Y., Xiong, Y. and Zhang, H. (2020) 'Physicochemical structure and reactivity of char from torrefied rice husk: Effects of inorganic species and torrefaction temperature', *Fuel*, 262, p. 116667.
42. Zheng, A., Zhao, Z., Chang, S., Huang, Z., Wang, X., He, F. and Li, H. (2013) 'Effect of torrefaction on structure and fast pyrolysis behavior of corncobs', *Bioresource Technology*, 128, pp. 370-377.